Effect of Methotrexate on the Cerebellar Cortex of Adult Male Albino Rats and the Possible Role of Thymoquinone (Histological and Immunohistochemical Study)

Original Article

Azza Saad Shehata, Samar Mahmoud Elwakeel, Samah M. Ahmed and Maha Zayed Mohammed

Department of Medical Histology & Cell Biology, Faculty of Human Medicine, Zagazig University, Zagazig, Egypt.

ABSTRACT

Background: Methotrexate (MTX) is an anti-metabolite most commonly used in chemotherapy and immunosuppressant in auto-immune diseases. It is one of the major choices to treat various types of cancers. Thymoquinone (TQ) is the principal component of Nigella sativa (N. Sativa). It has prominent therapeutic actions as it possesses antiapoptotic, antioxidant, antimicrobial, and, hepatoprotective activities.

Objective: This study aimed to clarify the possible effect of TQ on the histological changes of the cerebellar cortex of MTX -treated adult male albino rats. In addition, to assess the restoration of the normal histological structure after cessation of MTX.

Materials and Methods: Thirty six adult healthy male albino rats were divided into four groups; group I (Control group), group II (MTX group) received (0.5 mg/kg BW) MTX intraperitoneally (i.p.) twice a week for four weeks. Group III (MTX and TQ group) received MTX intraperitoneally similar to (group II) in concomitant with TQ orally at a dose of (10 mg/kg BW) dissolving in (1ml) distilled water daily for four weeks, and group IV (recovery group) received MTX intraperitoneally similar to (group II) then left without treatment for 15 days. At the end of the experiment, all rats were anesthetized and cerebellar specimens were obtained and processed for light and transmission electron microscope examination. Morphometric and statistical analyses were also performed.

Results: During the experiment, MTX group showed gradual deterioration of the motor activities and a statistically significant decrease in the body weight, Microscopic examination displayed shrunken Purkinje cells with darkly stained pyknotic nuclei. Cresyl fast violet-stained cerebellar sections showed ill-defined purple Nissl granules in the perikarya of Purkinje cells and other neurons.Immunohistochemical-stained sections for GFAP showed a strong positive reaction in the processes of astrocytes, weak positive reaction for Bcl-2 in neuronal cytoplasm. MTX and TQ-treated groups showed no deterioration in their motor activities. Most Purkinje cells had a pyriform shape, vesicular nuclei, and basophilic cytoplasm. Few Purkinje cells appeared irregular and darkly stained. Signs of degeneration were still present in the cerebellar cortex of the recovery group.

Conclusion: The cerebella of MTX- treated albino rats showed evident structural alterations seen by light and electron microscopes and also marked changes in the immunohistochemical reactions indicating its neurotoxicity. Co-administration of TQ attenuated these changes more than cessation of MTX. This indicates TQ neuroprotective effect which can be considered clinically.

Key Words: Cerebellum, methotrexate, thymoquinone.

Revised: 8 September 2023, **Accepted:** 8 November 2023.

Corresponding Author: Maha Zayed Mohammed, MD, Medical Histology & Cell Biology Department, Faculty of Human Medicine, Zagazig University, Zagazig,, Egypt, **Tel.:** 01090886200, **E-mail:** mahazayed676@gmail.com

ISSN: 2536-9172, June 2023, Vol. 7, No. 1

INTRODUCTION

Chemotherapy is a powerful form of drug therapy that effectively destroys the body's rapidly proliferating cells. It is mostly employed for lowering the overall number of cancer cells, reduce the spread of cancer, reduce the size of tumors, and decrease the signs and symptoms already present. This makes it the best choice for various cancer types.[1] MTX is used to treat many types of cancer including breast cancer, lung cancer, certain types of lymphoma and leukemia. It treats cancer by slowing the growth of cancer cells, but it has many side effects such as: excessive bleeding, diarrhea, fatigue, loss of appetite, nausea, vomiting, weight loss, infections, anemia, neuropathy, memory issues, concentration issues, skin changes, fertility changes and neurotoxicity [2]. These side effects are equivalent to those of a folate shortage, thus they can be avoided by supplementation of methotrexate with folic acid. Neurotoxicity is one of the major MTX adverse effects. On the other hand, it is effective in the treatment of many autoimmune diseases [3].

The incidence and severity of MTX neurotoxicity are principally related to its dose intensity and duration of treatment[4]. MTX can induce oxidative stress, mitochondrial swelling, cytochrome c release and an

 DOI: 10.21608/jmh.2023.235142.1119

increase in caspase 9, causing apoptosis. Furthermore, overexpression of pro-inflammatory factors such as nuclear factor kappa B (NF-κB) and interleukin 6 (IL-6) indicates MTX-induced inflammation[5].

Nigella sativa is a medicinal plant with strong traditional background. N. sativa seeds contain fixed oil, essential oil, alkaloids, proteins, and saponins. Its biologically active molecules are thymoquinone, flavonoids, α-hederin, antioxidants and fatty acids which are good for a healthy well-being[6]. Antioxidant, anti-inflammatory, anti-microbial, anti-epileptic, and anti-cancer properties are only a few of its medicinal effects. It could be a treatment for memory-affecting neurodegenerative diseases and brain injury.[7] Thymoquinone (TQ), the main component of essential oil obtained from N. sativa seeds, has a wide range of medicinal and pharmacological effects[8]. The potential of TQ against heavy metals, aflatoxins and carcinogens that induced oxidative damage was confirmed. This supports its use as a medication that has many applications in medicine. It is systemically well-tolerated with a large safety profile also; it has the potential to reduce systemic toxicity and oxidative stress. It is an excellent option for treating a variety of nerve lesions due to its less adverse effects, availability, and reasonable price compared to other synthetic drugs[9]. It was reported that TQ has a role in cancer management via the activation and inactivation of molecular cascades. It exhibits apoptosis of cancer cells through activation of tumor-suppressor gene, inhibition of transcription factor and inhibition of angiogenesis. Also, it is considered as an anti-proliferative agent [10].

Therefore, the purpose of the study was to determine the effect of MTX on the histological structure of the cerebellar cortex in adult male albino rats and to evaluate the influence of concomitant TQ administration on the histological changes and also to assess recovery after cessation of methotrexate.

MATERIALS AND METHODS

Animals

Thirty six healthy adult male albino rats (14 -18 weeks), ranging from -190-220 g- were used in this research. They were housed in clean properly ventilated cages with free access to food and water throughout the experiment. Rats were randomly divided into four groups and were given doses based on their body weight. This study was performed in Medical Histology and Cell Biology Department, Faculty of Medicine, Zagazig University. All experimental procedures were approved and performed in accordance with the guidelines for animal research issued by the National Institute of Health and were approved by the Animal Ethics Committee of the Faculty of Medicine, Zagazig University, Egypt, (ZU-IACUC/3/F/27/2020).

Chemicals:

Methotrexate: was obtained in the form of injections (50 mg/5ml) vial from Sandoz, Novartis scientific office.

Thymoquinone: was purchased from Sigma-Aldrich in the form of yellowish crystalline powder (1g) which is soluble in distilled water.

Experimental design:

Thirty six adult male albino rats were divided into four groups:

• **Control group (Group I):** included 18 rats that were subdivided into three equal subgroups (six rats each):

Subgroup Ia: rats were given no treatment.

Subgroup Ib: rats were given distilled water orally (as avehicle for TQ) at a dose of (1 ml/kg BW) daily for four weeks[11].

Subgroup Ic: rats were given TQ orally at a dose of (10 mg/kg BW) daily for four weeks via intragastric route, freshly prepared by dissolving in (1ml) distilled water [11].

• **MTX treated group (Group II):** six rats were intraperitoneally (i.p.) injected with MTX (0.5 mg/kg) twice a week for four weeks [12].

• **MTX and TQ treated group (Group III):** six rats were intraperitoneally (i.p.) injected with MTX (0.5 mg/kg) twice a week for four weeks[12] in concomitant with TQ orally at a dose of (10 mg/kg BW) daily for four weeks using the intragastric route. It was prepared freshly by dissolving in (1ml) distilled water[11].

• **MTX withdrawal group or recovery group (Group IV):** six rats were intraperitoneally (i.p.) injected with MTX (0.5 mg/kg) twice a week for four weeks then left without treatment for 15 days[13].

Experimental procedure

General observations:

The rats were assessed daily for motor activity, general health and the amount of food intake until the end of the study.

Body Weight:

An electrical balance was used to weigh each rat regularly (Sartorius Goetting type 140/AG, Berlin, Germany) starting from the beginning to the end of the experiment.

At the end of the experiment, the animals in all groups were anesthetized with an intraperitoneal injection of thiopental sodium (50mg/kg)[14]. The specimens from each group were processed for light and transmission electron microscopic study.

1) Light microscope:

After the chest wall was opened in rats processed for light microscope, rats were perfused with 10% formol saline. The skull was opened and the brain was removed. The cerebellum was carefully dissected, then, a midsagittal section of the cerebellar vermis was made, each cerebellum was cut into two equal portions, the first of which was fixed in 10% formaldehyde for light microscope examination and the second of which was chopped into small pieces (1 mm3) and rapidly fixed in 1% phosphate buffered glutaraldehyde, then processed for electron microscope study.

Light microscope examination:

After fixation, specimens were processed to obtain paraffin blocks, then, sections of 5µm thick were cut and stained with:

a- Haematoxylin and Eosin (H&E) stain: as a routine method for examining the cerebellar cortex's general histological structure.

b- Cresyl fast violet stain: to demonstrate Nissl's substance in the cytoplasm of neurons.

c- Immunohistochemical stain: paraffin sections were stained to test

• The protein expression of Glial Fibrillary Acidic Protein (GFAP): to demonstrate the astrocyte activity.

• Bcl-2: sections were immune-stained using the horseradish peroxidase (HRP) polymer conjugate technique; it is used as indicator for apoptosis.

2) Electron Microscope Examination:

Intracardiac perfusion in rats processed for electron microscopy was carried out with 2.5% glutaraldehyde, buffered in 0.1 ml phosphate buffer for 5 minutes for partial fixation of the brain. The skull was opened and the brain was removed. The cerebellum was excised and a midsagittal section of the cerebellar vermis was made. The cerebellar samples were rapidly removed and cut into small pieces about ($1mm^3$), fixed in 2.5% glutaraldehyde, buffered in 0.1 ml phosphate buffer at 4ºC and post-fixed in 1% osmium tetroxide. Then, they were dehydrated in ascending grades of alcohol, embedded in resin and sectioned by ultramicrotome to prepare:

a- The thick sections (0.5-1µm thick) were mounted on glass slides and stained with toluidine blue. They were used as a guide for ultra-thin sections.

b- The thin sections (ultra-thin sections) that were examined under electron microscope.

Examination and photography were done by JEOL JEM 1010 electron microscope in the Regional Center of Mycology and Biotechnology (RCMB), Mansoura University, Egypt.

3) - Image Analysis and Morphomertic study:

Included:

- The number of Purkinje cells in H&E- -stained sections

- Optical density of cresyl fast violet staining

- The area percentage of GFAP

- The area percentage of Bcl-2 immunoreactivity.

Then, sections were morphometrically analyzed using image analyzer computer system. Image analysis was done using Leica Microsystems LTD (DFC 295) software image analysis computer system (Germany) in the Dentistry Research and Equipment Unit, Faculty of Dentistry, Cairo University.

4)- Statistical analysis:

The morphometric data were analyzed using one-way analysis of variance (ANOVA) for comparison between the different groups (more than two groups) followed by least significance difference test (LSD)[15].

RESULTS

General Observations:

During the experiment, the animals of the control groups subgroup (Ia, subgroup Ib, and subgroup Ic) showed an excellent general health. with normal physical and motor activity and good appetite and were awake and alert. Group II (methotrexate-treated group), the animals suffered from a progressive decrease in their appetites. They were weak and lethargic. Their motor activity revealed considerable deterioration during the experiment. On the other hand, the rats which received both MTX and TQ showed better general condition and motor activity than the methotrexate-treated group. Animals of the recovery group revealed slight gradual improvement in their motor activity and appetites. They were weak and lethargic.

Body weight:

Similar body weights and histological results of all the control subgroups (Ia, Ib and Ic) were obtained, so results of all subgroups were combined and interpreted as a single control group for statistical analysis. There was a statistically significant difference in body weight between the different studied groups (*p-value < 0.001*) with the highest weight in the control group (214± 3.6) and the lowest one in MTX treated group (192.33 ± 4.04). MTX &TQ treated group was (216 ± 6.08) and the recovery group was (204 ± 2.02). (Tables 1a &1b).

Mortality rate:

Four deaths occurred in the (methotrexate treated group) and two deaths in the (recovery group). These rats were excluded from the experiment.

B) Histological results:

A-Light microscope examination:

• Hematoxylin and eosin:

- Histological examination of cerebellar cortex sections of subgroup Ia, Ib and Ic showed nearly the same histological structure, so subgroup Ia was referred as the control group. H&E-stained sections in the cerebellar cortex of the control group showed normal architecture. It was composed of three layers; an outer molecular layer containing small stellate cells and basket cells, a middle Purkinje cell layer containing a single row of Purkinje cells and an inner granule cell layer containing numerous closely packed granule cells with few Golgi cells (Figs. 1a & 1b). The methotrexate-treated group showed vacuolations in the molecular layer. Purkinje cell layer appeared disrupted, shrunken and deeply stained. Other cells displayed total degeneration with vacuolated cytoplasm and no nuclei. The granule cell layer showed shrunken deeply stained granule cells (Fig. 1c). Methotrexate and thymoquinone-treated cerebellum showed small stellate cells and basket cells in the outer molecular layer. In the middle layer, Purkinje cells were arranged in a single row with pale vesicular nuclei, prominent nucleoli and basophilic cytoplasm. Bergmann astrocytes were seen loosely related to Purkinje cells. The granule cell layer contained small granule cells with deeply stained nuclei and Golgi cells with large pale nuclei (Fig.1d).

- The cerebellum of the recovery group showed persistence of cellular degeneration. Small stellate cells and basket cells were detected in the molecular layer, while in the Purkinje cell layer, some Purkinje cells, were pyriform in shape with vesicular nuclei and prominent nucleoli, but most cells appeared shrunken with deeply stained nuclei. The granule cell layer consisted of granule cells containing heterochromatic nuclei bordered by a thin rim of cytoplasm. Golgi cells contained large pale nuclei (Fig.1e).

• Cresyl fast violet:

- Sections of the control group revealed cytoplasmic purple Nissl granules arranged as a ring around their nuclei in Purkinje cells (Fig. 2a).

-Methotrexate treated group showed irregular densely stained Purkinje cells with ill-defined cytoplasmic purple Nissl granules (Fig. 2b).

- Methotrexate and thymoquinone treated group showed purple Nissl granules arranged as a ring around the nuclei of Purkinje cells (Fig. 2c).

- In the recovery group, purple Nissl granules were noticed in the perikarya of some Purkinje cells, but most cells were densely stained with ill-defined Nissel substance (Fig. 2d).

Immunohistochemical stains:

• Immunoperoxidase reaction for GFAP:

- In the cerebellar cortex of the control group, the astrocytes cytoplasm and processes showed positive immunoreaction (Fig. 3a).

- In the methotrexate treated group, the cytoplasm and processes of astrocytes in all layers of cerebellar cortex displayed an increase in the intensity of positive reaction for GFAP (Fig. 3b).

- Methotrexate and thymoquinone treated group revealed positive immunoreaction in the cytoplasm and processes of astrocytes in all layers of the cerebellar cortex (Fig. 3c).

- In the recovery group, there was an increase in intensity and number of positive reaction in the cytoplasm and processes of astrocytes in all layers of the cerebellar cortex (Fig. 3d).

• The immunoperoxidase reaction for Bcl-2:

- In the control cerebellar sections, the cytoplasm of Purkinje and basket cells showed strong positive reaction (Fig. 4a).

- Methotrexate treated group revealed negative cytoplasmic reaction for Bcl-2 in most Purkinje cells and basket cells (Fig. 4b).

- In the methotrexate and thymoquinone treated group, a positive reaction was seen in the cytoplasm of some Purkinje cells and Basket cells (Fig. 4c).

- The recovery group revealed negative cytoplasmic reaction for Bcl-2 in Purkinje cells and basket cells (Fig. 4d).

• *Examination of semithin sections stained with toluidine blue:*

- The control cerebellar cortex: Purkinje cell layer with pyriform to rounded cells having large vesicular nuclei and deeply basophilic cytoplasm containing Nissl granules. Pale-stained Bergmann astrocytes were seen closely related to Purkinje cells. In the granule cell layer, granule cells appeared densely packed and have oval nuclei with peripheral clumps of heterochromatin and a thin rim of cytoplasm. The cerebellar islands (glomeruli) appeared as rounded basophilic areas intertwined between granule cells (Fig. 5a). Methotrexate treated group showed molecular layer with small population of cells. Purkinje cell layer contained irregular shrunken Purkinje cells having dark nuclei and deeply stained cytoplasm with decreased staining intensity for Nissl granules. Pale-stained Bergmann astrocytes with irregular contours were observed closely related to Purkinje cells. In the granule cell layer, granule cells had slightly irregular nuclei with peripheral heterochromatin clumps and a thin rim of cytoplasm. Congested blood vessel was also observed in granule cell layer (Fig. 5b). In methotrexate and thymoquinone -treated group most purkinje cells appeared pyriform to rounded having large vesicular nuclei with prominent nucleoli. Nissl granules were intensely stained. Pale-stained Bergmann astrocytes were seen closely related to Purkinje cells. In the granule cell layer, granule cells had oval nuclei with peripheral heterochromatin clumps and a thin rim of cytoplasm (Fig. 5c). Recovery group showed a molecular layer formed of nerve fibers and a small population of cells. Purkinje cell layer contained irregular shrunken Purkinje cells having darkly stained nuclei and deeply stained cytoplasm whereas Nissl granules staining showed decreased intensity of. Pale-stained Bergmann cells with slightly irregular contours were seen closely related to Purkinje cells. In the granule cell layer, some cells contained a thin rim of cytoplasm with heterochromatic nuclei and others appeared darkly stained with pyknotic nuclei (Fig. 5d).

B-Transmission Electron Microscopic Examination: Examination of ultrathin sections showed:

- The molecular layer of the control cerebellar cortex contained intact myelinated nerve fibers of the molecular layer (Fig. 6a).

- MTX-treated group showed some nerve fibers in the molecular layer with intact myelin sheaths while others showed separation of their myelin sheaths (Fig. 6b).

- The molecular layer of methotrexate and thymoquinone treated group displayed intact myelinated nerve fibers (Fig. 6c).

- The cerebella of the recovery group exhibited that degenerative changes were still present. Most nerve fibers of molecular layer appeared myelinated and intact (Fig. 6d).

- Purkinje cells of the control group contained euchromatic nuclei and electron dense cytoplasm contained multiple mitochondria. The glial cells (Bergmann astrocytes) were seen closely related to Purkinje cells and appeared with euchromatic nucleus (Figs. 7a).

- Purkinje cells of the MTX-treated group were irregular and contained dark nuclei enclosed in irregular pleated nuclear membranes .The cisternae of the rough endoplasmic reticulum were dilated (Fig. 7b).

- The outlines of Purkinje cells of the recovery group were still irregular. Their nuclei were shrunken with prominent nucleoli and irregular and crinkled membranes . In the cytoplasm Golgi apparatus saccules and dilated cisternae of rough endoplasmic reticulum were seen (Fig. 7d).

- The granule cell layer of the MTX-treated group showed different degrees of degeneration of granule cells. Some cells had rounded regular nuclei with clumped heterochromatin.others were shrunken with dark shrunken nuclei containing clumped heterochromatin. Other cells appeared small with dark pyknotic nuclei and vacuolated cytoplasm. Neuroglia cells mostly-oligodendroglia-contained electron-dense cytoplasm and heterochromatic irregular nuclei. Distorted and dissociated myelin sheaths of the nerve fibers were also observed (Fig. 8b).

- The methotrexate and thymoquinone treated group showed most granule cells with heterochromatic nuclei bordered by a thin rim of cytoplasm containing multiple mitochondria and free ribosomes. The other granule cells looked smaller with shrunken darkly stained nuclei. A glial cell-mostly oligodendroglia -with a heterochromatic nucleus and dense cytoplasm was observed. A nerve fiber with intact myelination was also observed. (Fig. 8c).

- Granule cells in the granule cell layer of the recovery group showed heterochromatic nuclei and a thin rim of cytoplasm. A neuroglia cell -mostly oligodendroglia-was also observe electron-densen dense cytoplasm. Disrupted, dissociated myelin sheaths of the nerve fibers were visible (Fig. 8d).

C) Morphometric Results:

Mean number of Purkinje cells:

By using one way ANOVA test, statistical analysis of the mean value of Purkinje cells number revealed statistically significant difference among the different studied groups as the *P value < 0.001*** with the highest number in the control group (15.078±1.25) and least one in the MTX treated group (4.38 ±0.988). Least significance difference was calculated for comparison between the five groups and revealed statistically significant increase in number of Purkinje cells in (control group) compared to group II (MTX treated) and group IV(Recovery) while there was no significant difference between the control group and group III (combined MTX&TQ). In addition, a statistically significant decrease in the mean number of Purkinje cells was recorded in group II (MTX treated) and group IV (Recovery) compared to the other groups. On the other hand, there was non-significant difference between group II (MTX treated) and group IV (Recovery) (Tables 2a, 2b).

Optical Density of cresyl fast violet staining:

By using one way ANOVA test, statistical analysis of the mean value of optical density of cresyl fast violet staining revealed statistically significant difference among the studied groups as the *P value < 0.001*** with the highest level in the control group (60.34±1.78) and lowest one in the MTX treated group (40.71±1.77). Least significance difference was calculated for comparison between the five different groups and revealed statistically significant increase in density in (control group) compared to group II (MTX treated) and group IV (Recovery) while there was no significant difference between control group and (MTX&TQ treated group). Also, statistically significant decrease in optical density level in group II (MTX treated) and group IV (Recovery) compared to the other groups. However, there was non-significant difference between group II (MTX treated) and group IV (Recovery) (Tables 3a, 3b).

Area% of GFAP Immune reaction:

By using one way ANOVA test, statistical analysis of the mean value of area% of GFAP revealed statistically significant difference among the different studied groups as the *P value < 0.001*** with the highest level in MTX treated group (39.36±7.93) and lowest level in control group (9.71±3.78). Least significance difference (LSD) was calculated for comparison between groups and revealed statistically significant decrease in GFAP level in (control group) compared to group II (MTX treated) and group IV (Recovery) while there was no significant difference between control group and group III (MTX &TQ treated). Also, statistically significant increase in GFAP level in group II (MTX treated) when compared with the other groups (Tables 4a, 4b).

Area% of Bcl-2 Immune reaction:

Statistical analysis of the mean value of area % of Bcl-2 immune reaction using one way ANOVA test revealed statistically a significant difference among the different studied groups as the *P value < 0.001*** with the highest level in the control group (27.28±8.25) and the lowest level in MTX-treated group (2.42±0.68). The least significance difference was calculated for comparison between the five studied groups and revealed a statistically significant increase in Bcl-2 level in (control group) compared to group II (MTX-treated) and group IV (Recovery group) while there was no significant difference between the control group and group III (MTX& TQ treated). Also, a statistically significant decrease in Bcl-2 level in group II (MTX-treated) and group IV (Recovery) compared to the other groups. However, there was a non-significant difference between group II (MTX-treated) and group IV (Recovery) (Tables 5a, 5b).

Table (1) a: Comparing weight of rats among the studied groups.

Groups	Mean±SD Initial body weight	Mean±SD Weight at the end of experiment	F- test	*P-value*
Control group	201±3.741	214± 3.6		
MTX treated group	198.7±5.71	192.33 ± 4.04	265.58	<0.001**
MTX&TQ treated group	196.8±5.91	216 ± 6.08		
Recovery group	203.7±10.21	204 ± 2		

F-test=ANOVA test

Table (1) b: LSD for comparison between groups:

	Control group	MTX treated group	MTX&TQ treated group	Recovery group
MTX treated group	<0.001**		<0.001**	NS
MTX &TQ treated group	NS	<0.001**		<0.05*
Recovery group	<0.001**	NS	<0.05*	

LSD=least significance difference
** *P< 0.001* Highly statistically significant difference
* *P>0.05* Statistically significant difference
NS *P >0.05* No statistically significant difference

Table (2) a: comparing mean number of purkinje cells among different groups:

Groups	Mean±SD	F	*P value*
Control group	15.078±1.25	36.58	0.001**
Methotrexate treated group	4.38 ±0.988		
Methotrexate+ thymoquinone treated group	12.769±0.79		
Recovery group	9.692±0.862		

F-test=ANOVA test

Table (2) b: LSD for comparison between groups:

	Control group	MTX treated group	MTX&TQ treated group	Recovery group
MTX treated group	<0.001**		<0.001**	NS
MTX &TQ treated group	NS	<0.001**		<0.05*
Recovery group	<0.001**	NS	<0.05*	

LSD=least significance difference
** *P< 0.001* Highly statistically significant difference
* *P>0.05* Statistically significant difference
NS *P >0.05* No statistically significant difference

Table (3) a: comparing optical density of cresyl fast violet staining between the different studied groups:

Groups	mean±SD	F	*P value*
Control group	60.341.78±	144.23	<0.001**
Methotrexate treated group	40.711.77±		
Methotrexate& thymoquinone treated	58.132.06±		
Recovery group	42.961.91±		

F-test=ANOVA test

Table (3)b: LSD for comparison between groups:

	Control group	MTX treated group	MTX&TQ treated group	Recovery group
MTX treated group	<0.001**		<0.001**	NS
MTX&TQ treated group	NS	<0.001**		<0.05*
Recovery group	<0.001**	NS	<0.05*	

LSD=least significance difference
***P <0.001* Highly statistically significant difference
**P <0.05* Statistically significant difference
NSP *>0.05* No statistically significant difference

Table (4) a: comparing Area% of GFAP immune reaction among the studied groups:

Groups	Mean±SD	F-test	*P- value*
Control group	9.71±3.78	45.24	<0.001**
Methotrexate treated group	39.36±7.93		
Methotrexate& thymoquinone treated group	12.19±3.34		
Recovery group	22.73±1.8		

F-test=ANOVA test

Table (4)b: LSD for comparison between different groups:

	Control group	MTX treated group	MTX&TQ treated group	Recovery group
MTX treated group	<0.001**		NS	NS
MTX&TQ treated group	NS	NS		<0.05*
Recovery group	<0.001**	<0.05*	<0.05*	

LSD=least significance difference.
***P <0.001* Highly statistically significant difference
**P <0.05* Statistically significant difference
NSP *>0.05* No statistically significant difference

Table (5) a: comparing Area % of Bcl-2 levels among the different studied groups:

Groups	Mean±SD	F-test	*P- value*
Control group	27.28±8.25	19.06	<0.001**
Methotrexate treated group	2.42±0.68		
Methotrexate& thymoquinone treated group	18.27±6.11		
Recovery group	8.34±3.12		

F-test=ANOVA test

Table (5)b: LSD for comparison between groups:

	Control group	MTX treated group	MTX&TQ treated group	Recovery group
MTX treated group	<0.001**		<0.001**	NS
MTX&TQ treated group	NS	<0.001**		<0.05*
Recovery group	<0.001**	NS	<0.05*	

LSD=least significance difference
** *P< 0.001* Highly statistically significant difference
* *P>0.05* Statistically significant difference
NS *P >0.05* No statistically significant difference

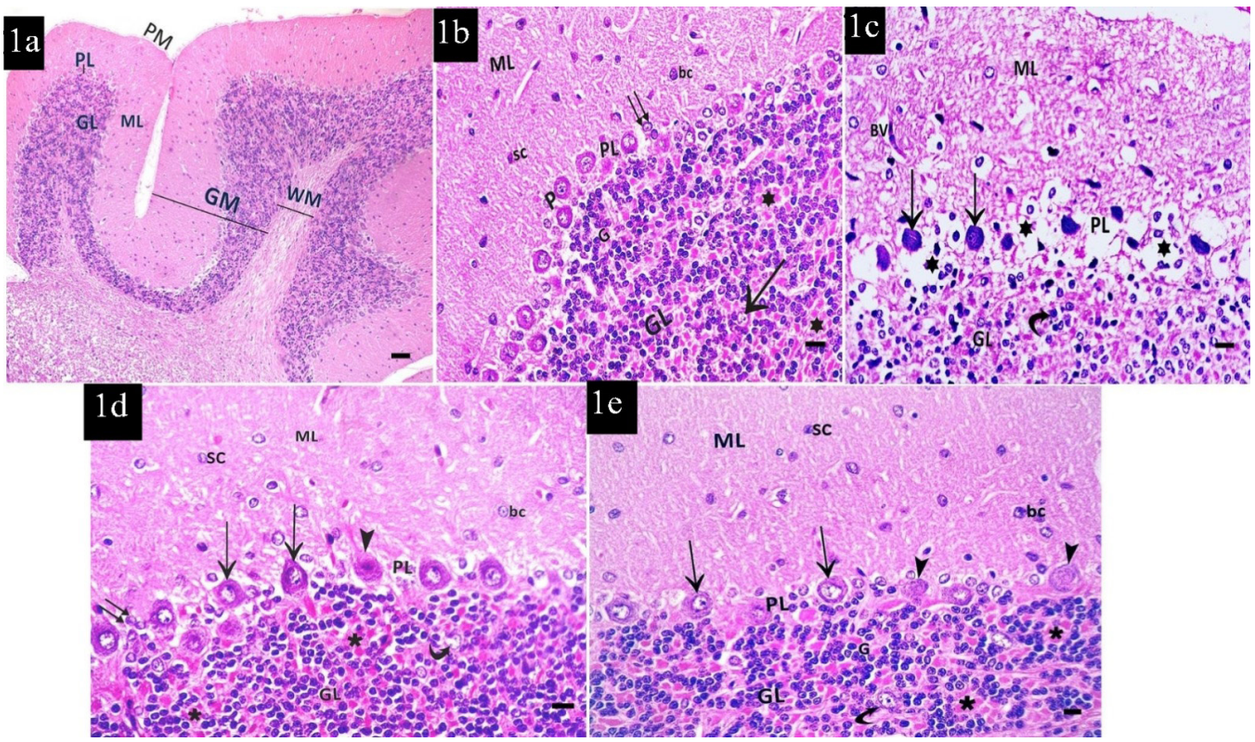

Fig. 1a: A photomicrograph of a section in the cerebellum of the control group showing cerebellar folium covered by pia mater (PM) and has outer cortex; grey matter (GM) and an inner medulla; white matter (WM). Cortex is formed of three layers; outer molecular layer (ML), middle Purkinje cell layer (PL) and inner granule cell layer (GL). (H& E × 100 - scale bar 20 µm).

Fig.1b: Control cerebellar cortex showing nerve cells of the molecular layer (ML); small stellate cells (sc), they are elliptical in shape with scanty cytoplasm and occupied almost entirely with rounded nucleus and basket cells (bc) which are round with large oval nucleus. The middle Purkinje cell layer (PL) consists of a single row of large pear shaped cells Purkinje cells (P) with pale vesicular nuclei and basophilic cytoplasm. Bergmann astrocytes (double arrows) are seen closely related to Purkinje cells. The granule cell layer (GL) consists of numerous small closely packed granule (G) cells with deeply stained nuclei and Golgi cells (arrow) which are large with vesicular nuclei. Glomeruli (cerebellar islands) (stars) are observed as acidophilic areas intertwined between granule cells (H&Ex400 - scale bar 10 µm).

Fig. 1c: MTX treated cerebellar cortex showing molecular layer with multiple vaculations (stars). Blood vessel (BV) is also observed in the molecular layer. Purkinje cell layer (PL) is disrupted. Shrunken deeply stained Purkinje cells (arrows) with deep homogenous cytoplasm and absence of Nissl granules with pyknotic nuclei are seen. In the granule cell layer (GL), the granule cells appear shrunken and deeply stained (curved arrow). (H & E × 400- scale bar 10 µm).

Fig.1d: MTX and TQ treated group cerebellar cortex showing nerve cells of the molecular layer (ML); small stellate cells (sc) which are elliptical in shape with scanty cytoplasm and occupied almost entirely with rounded nucleus & basket cells (bc) which are round with large oval nucleus. The middle Purkinje cell layer (PL) consists of a single row of large pear shaped cells Purkinje cells (P) with pale vesicular nuclei, prominent nucleolus and basophilic cytoplasm. Bergmann astrocytes (double arrows) are seen closely related to Purkinje cells. Granule cell layer (GL) contains densely populated small granule cells with deeply stained nuclei and thin rim of cytoplasm. Golgi cell (curved arrow) with pale nucleus is also observed (H & E × 400- scale bar 10 µm).

Fig.1e: Cerebellar crtex of the recovery group showing nerve cells in the molecular layer (ML); small stellate cells (sc) occupied almost entirely with rounded nucleus and basket cells (bc) with large oval nucleus. Purkinje layer (PL) contains some Purkinje cells (arrow) pyriform in shape with vesicular nuclei and prominent nucleoli, but most cells appear shrunken with deeply stained nuclei (arrow head). The granule cell layer (GL) consists of granule cells (G) with heterochromatic nuclei. A golgi cell (curved arrow) appear with large pale nucleus. (H & E × 400- scale bar 10 µm).

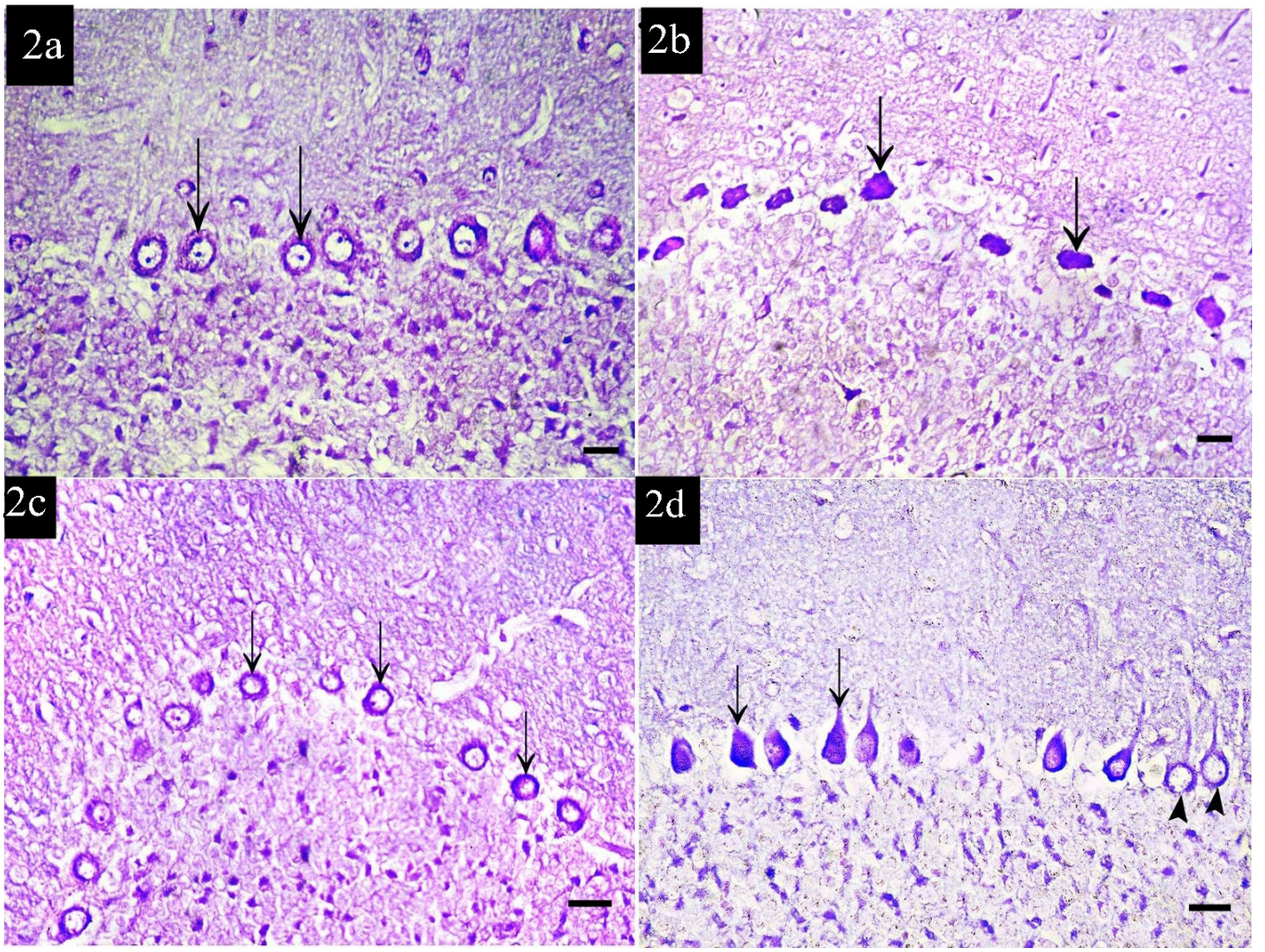

Fig. 2a: Examination of cresyl fast violet stained cerebellar sections of the control group showing purple Nissl granules in the cytoplasm of Purkinje cells that appear as a ring around their nuclei (arrow).
Fig. 2b: Methotrexate-treated group showing irregular densely stained Purkinje cells with ill-defined purple Nissl granules in their perikarya (arrow).
Fig. 2c: Methotrexate and thymoquinone-treated group showing purple Nissl granules in the perikarya of Purkinje cells (arrow).
Fig. 2d: In the recovery group, purple Nissl granules in the perikarya of some Purkinje cells (arrowhead) are noticed, but most cells are densely stained with ill-defined Nissel's substance in the perikarya of Purkinje cells (arrow). (Cresyl fast violet× 400- scale bar 10 μm).

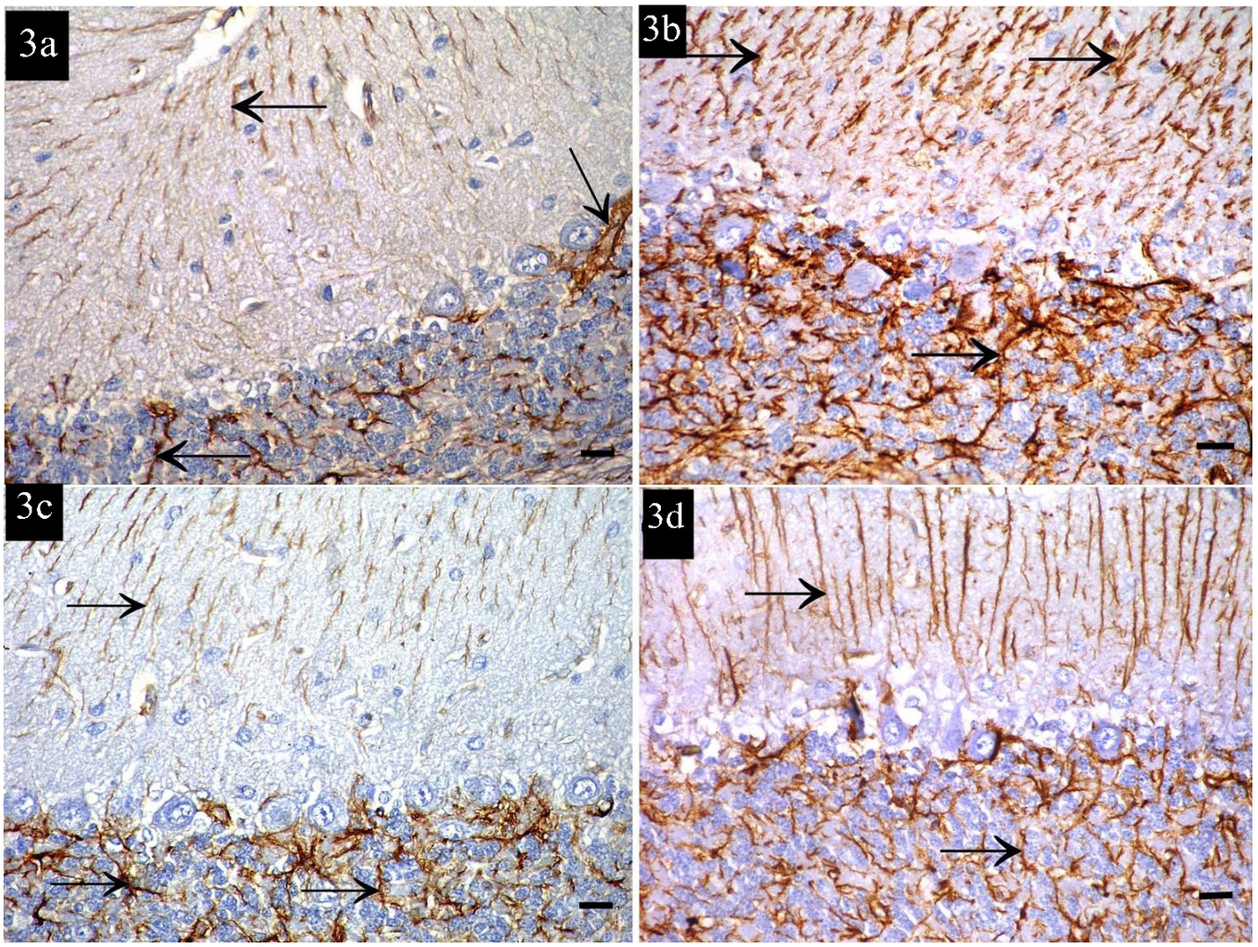

Fig. 3a: Immunoperoxidase reaction for GFAP of the control group shows positive immunoreaction in the cytoplasm and processes of astrocytes in the cerebellar cortex (arrow).
Fig.3b: In the methotrexate treated group, there is increase in the intensity of the positive reaction for GFAP in the cytoplasm and processes of astrocytes in all layers of the cerebellar cortex (arrow).
Fig.3c: Immunoperoxidase reaction for GFAP of methotrexate and thymoquinone treated group reveals a positive immunoreaction in the cytoplasm and processes of astrocytes in layers of cerebellar cortex (arrow).
Fig. 3d: In the recovery group, an increase in the intensity and number of positively reacting cells in the cytoplasm and processes of astrocytes in all layers of cerebellar cortex are seen (arrow). (Immunoperoxidase reaction for GFAP × 400- scale bar 10 μm)**.**

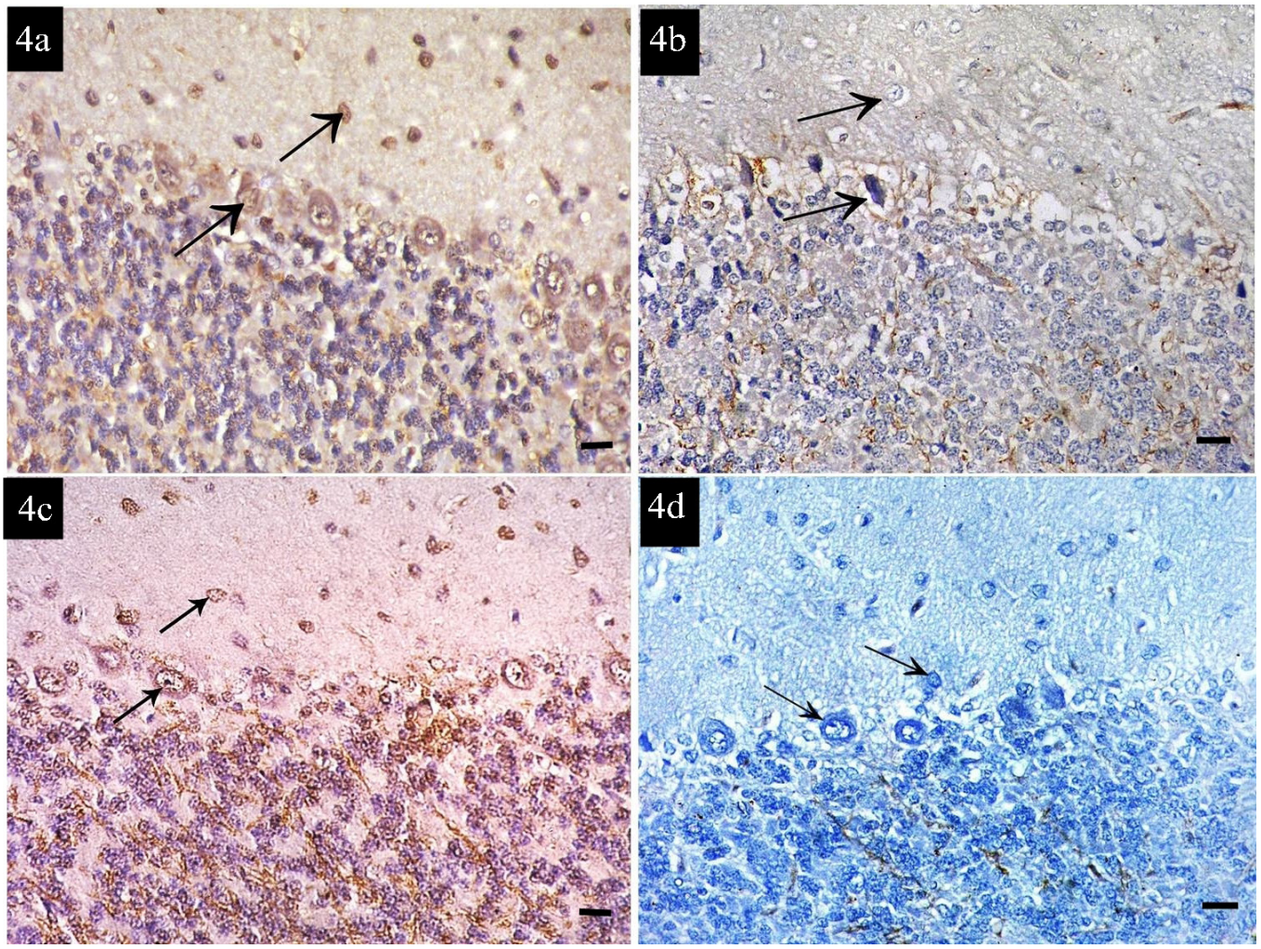

Fig. 4a: The immunoperoxidase reaction for Bcl2 of the control cerebellar sections showing a strong positive reaction in the cytoplasm of Purkinje and basket cells (arrow).
Fig.4b: Methotrexate-treated group reveals a negative reaction for Bcl-2 in the cytoplasm of most Purkinje cells and basket cells (arrow).
Fig. 4c: In methotrexate and thymoquinone-treated group, a positive reaction in the cytoplasm of some Purkinje cells and Basket cells (arrow) is seen.
Fig. 4d: Bcl-2 immunoperoxidase reaction of the recovery group reveals a negative reaction for Bcl-2 in the cytoplasm of Purkinje cells and basket cells (arrow). (Immunoperoxidase reaction for Bcl-2 × 400- scale bar 10 µm).

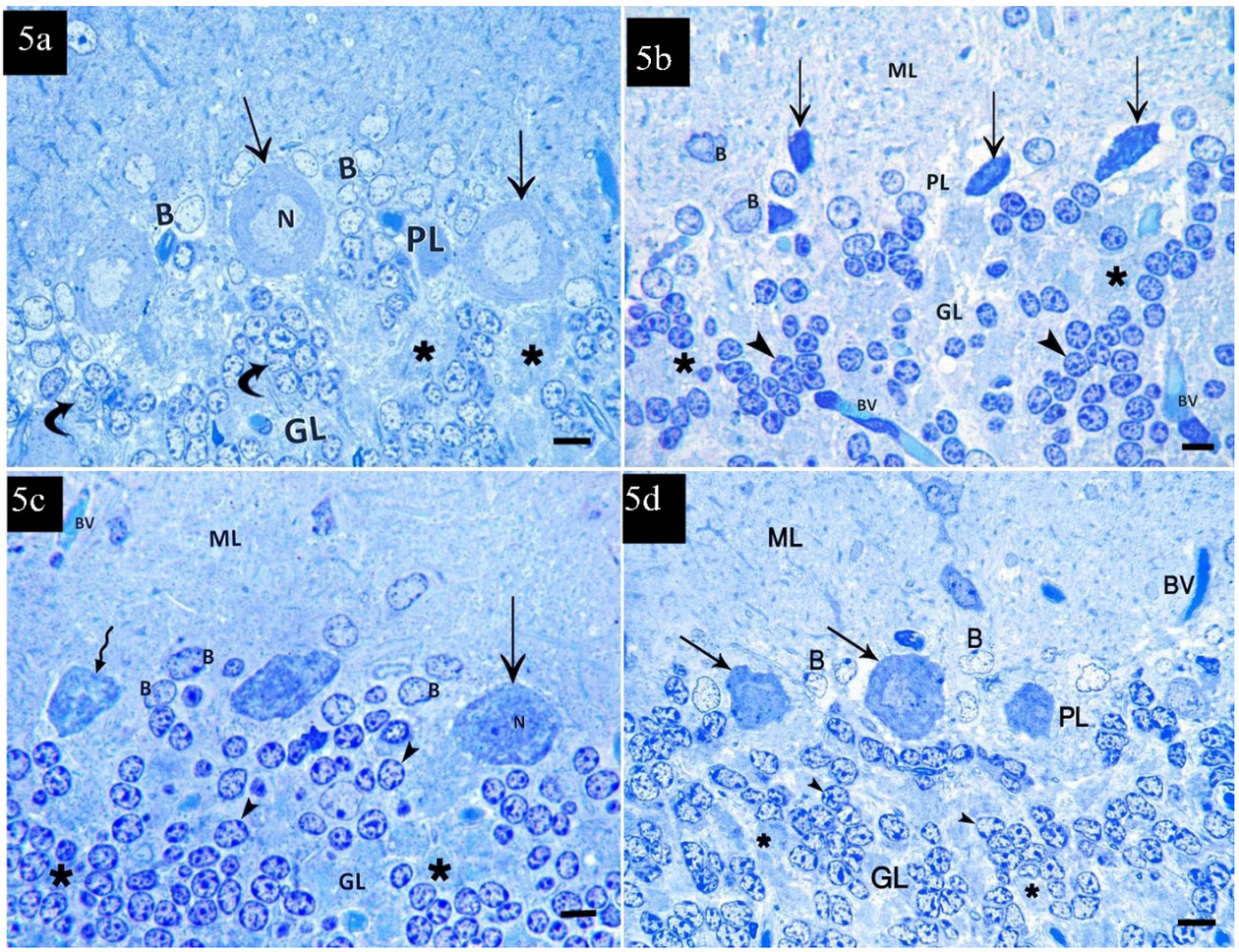

Fig. 5a: A photomicrograph of a semithin section in the control cerebellar cortex showing Purkinje cell layer (PL) with pyriform to rounded Purkinje cells (arrows) having large vesicular nuclei and dark blue cytoplasm. Pale-stained Bergmann astrocytes (B) are seen closely related to Purkinje cells. In the granule cell layer (GL), granule cells (curved arrow) appear densely packed and have oval nuclei with peripheral clumps of heterochromatin and a thin rim of cytoplasm. The cerebellar islands (glomeruli) (stars) appear as rounded basophilic areas intertwined between granule cells.

Fig. 5b: A photomicrograph of a semithin section in the MTX-treated cerebellar cortex showing the molecular layer (ML). Purkinje cell layer (PL) contains irregular shrunken Purkinje cells (arrows) having dark stained nuclei and dark-stained cytoplasm with decreased intensity of Nissl's granules stain. Pale-stained Bergmann astrocytes (B) with irregular contour are seen closely related to Purkinje cells. In the granule cell layer (GL), granule cells (arrow head) appear having slightly irregular nuclei with peripheral clumps of heterochromatin and surrounded with thin rim of cytoplasm. Congested blood vessel (BV) is also observed in granule cell layer.

Fig. 5c: A photomicrograph of a semithin section in MTX and TQ-treated cerebellar cortex showing a blood vessel (BV) that is noticed in the molecular layer (ML). Most Purkinje cells (arrow) appear pyriform to rounded having large vesicular nuclei (N) with prominent nucleoli and deep-stained cytoplasm. Purkinje cell with irregular outlines is also seen (zigzag arrow). Pale-stained Bergmann astrocytes (B) are seen closely related to Purkinje cells. In the granule cell layer (GL), granule cells (arrowhead) have oval nuclei with peripheral clumps of heterochromatin and a thin rim of cytoplasm. The cerebellar islands (glomeruli) (stars) appear intertwined between granule cells.

Fig. 5d: Recovery group showing molecular layer (ML) formed of nerve fibers and small population of cells. Purkinje cell layer (PL) contains irregular shrunken Purkinje cells (arrow) having dark stained nuclei and dark stained cytoplasm with decreased intensity of Nissl's granules. Pale-stained Bergmann astrocytes (B) with slightly irregular contours are seen closely related to Purkinje cells. In the granule cell layer (GL), some granule cells appear with heterochromatic nuclei and a thin rim of cytoplasm (arrowhead). The cerebellar islands (glomeruli) (stars) appear entangled between granule cells. (Toluidine blue x1000- scale bar 30 µm).

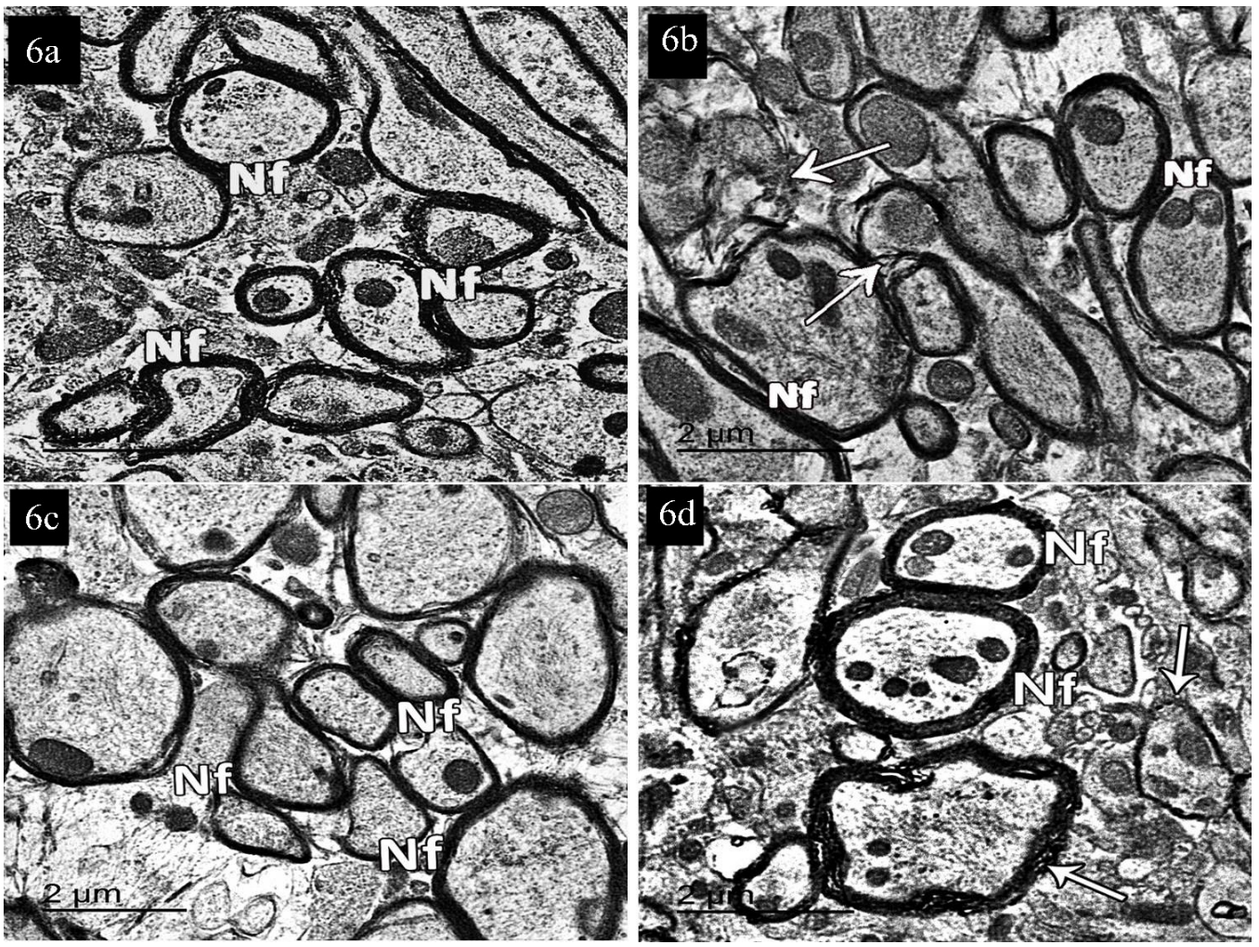

Fig. 6a: Transmission electron micrograph of an ultrathin section in the control cerebellar cortex of the molecular layer showing intact myelinated nerve fibers (Nf) of the molecular layer.
Fig. 6b: Ultrathin sections of the MTX-treated group showing some nerve fibers in the molecular layer with intact myelin sheath (Nf) while others show separation of their myelin sheaths (arrow).
Fig. 6c: Methotrexate and thymoquinone-treated group showing the molecular layer with intact myelinated nerve fibers (Nf).
Fig. 6d: Examination of ultrathin sections in the cerebellar cortex of the recovery group showing that some nerve fibers have degenerative changes (arrow). Most nerve fibers of the molecular layer are myelinated and intact (Nf).

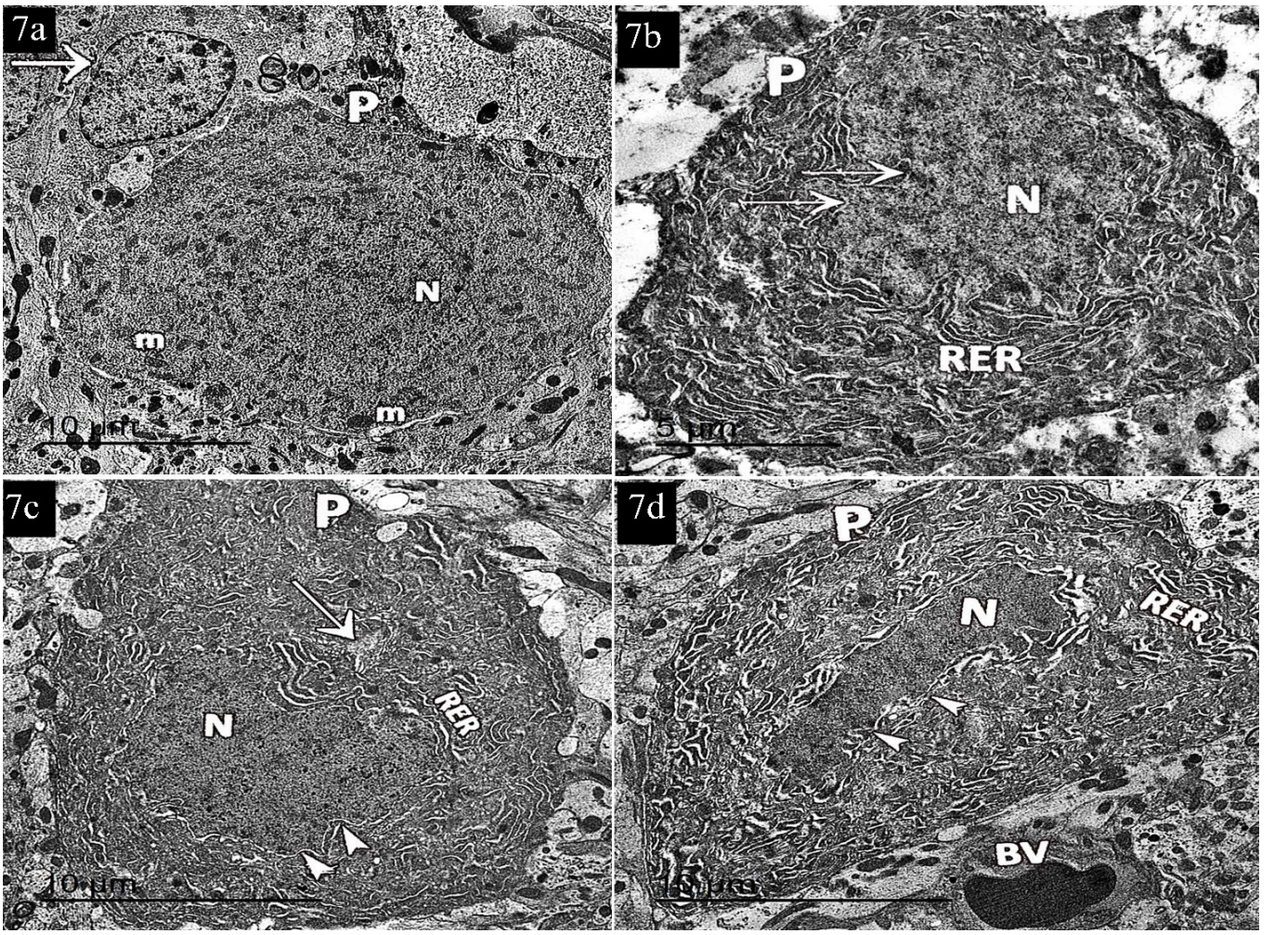

Fig.7a: Transmission electron micrograph of an ultrathin section in the control cerebellar cortex showing Purkinje cell (P) with euchromatic nucleus (N) and electron dense cytoplasm contains multiple mitochondria (m). Bergmann astrocyte (arrow) is seen closely related to Purkinje cell and contain euchromatic nucleus.

Fig.7b: Purkinje cell (P) of MTX-treated group shows irregular outline. The nucleus (N) is dark and irregular. The nuclear membrane (arrow) is indented and creased. Cytoplasm contains dilated cisternae of rough endoplasmic reticulum (RER).

Fig.7c: Methotrexate and thymoquinone treated group showing Purkinje cell (P) with more or less regular contour and large euchromatic nucleus (N). Nuclear membrane (arrow head) appears slightly irregular. The cytoplasm contained dilated cisternae of rough endoplasmic reticulum (RER) and Golgi apparatus saccules (arrow).

Fig.7d: Purkinje cell (P) of the recovery group appears with irregular contour. The nucleus (N) appears shrunken with a prominent nucleolus. The nuclear membrane (arrowhead) is irregular and creased. Cytoplasm had dilated cisternae of rough endoplasmic reticulum (RER). Blood vessel (BV) is also present.

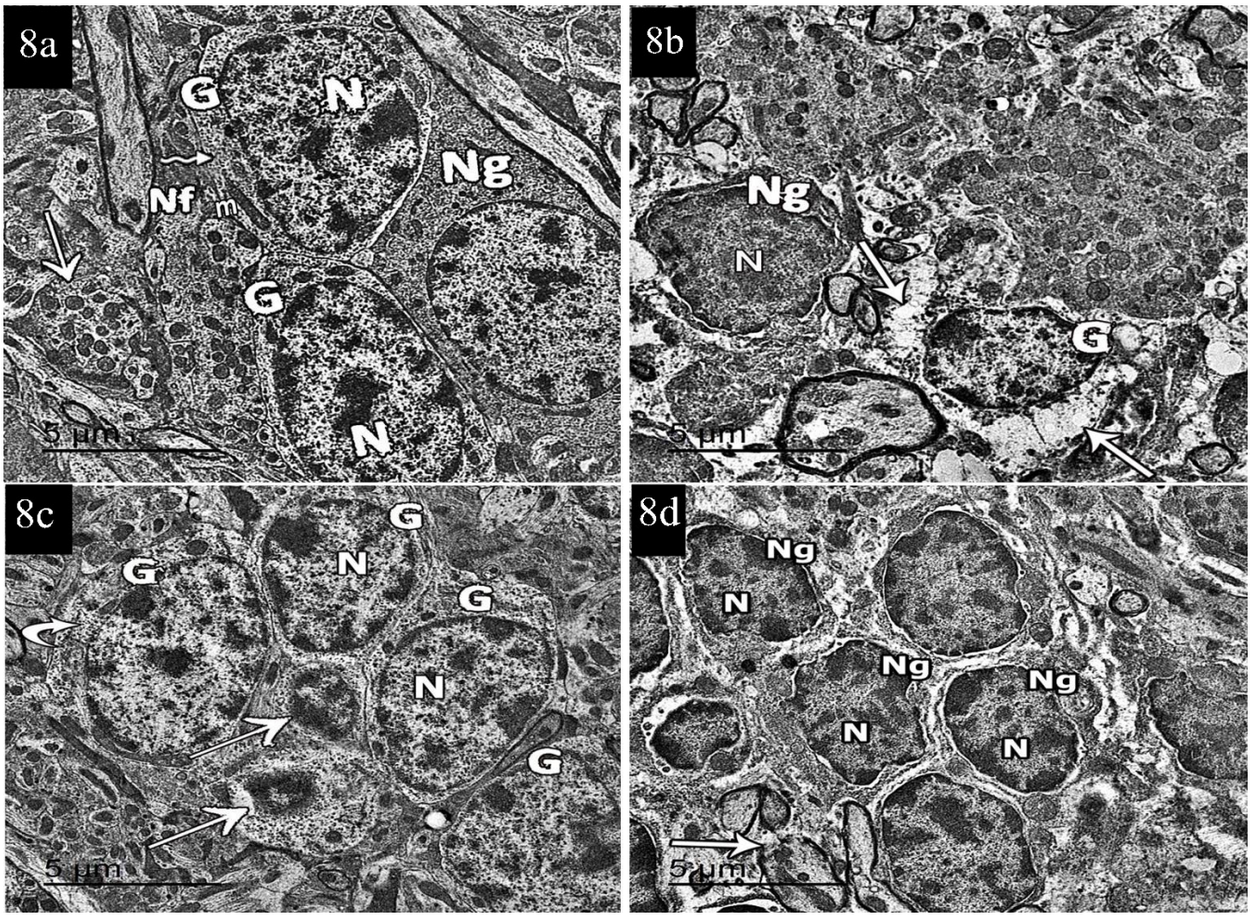

Fig. 8a: The granule cell layer of the control group shows small numerous granule cells (G) having oval euchromatic nuclei (N) with heterochromatic clumps. The cytoplasm has multiple free ribosomes (zigzag arrow) and mitochondria (m). A glial cell mostly oligodendrocyte (Ng) appears with electron-dense cytoplasm. The surrounding neuropil contains islands of interconnected myelinated (Nf) and unmyelinated nerve fibers (arrow).

Fig. 8b: The granule cell layer of MTX-treated group shows shrunken granule cell (G) with pyknotic nucleus and vacuolated cytoplasm (arrow). Neuroglia cell (Ng) contains dark heterochromatic nucleus (N).

Fig. 8c: Methotrexate and thymoquinone treated group showing most granule cells (G) with oval nuclei (N) and thin rim of cytoplasm containing free ribosomes (curved arrow). Other granule cells (arrow) appear smaller and have shrunken dark stained nuclei.

Fig. 8d: Granule cell in the granule cell layer of recovery group appears between neuroglia cells (Ng) mostly oligodendroglia that have heterochromatic nuclei (N) electron dense cytoplasm. Disrupted, dissociated myelin sheath of nerve fiber (arrow) is noticed.

DISCUSSION

Methotrexate (MTX) is a cytotoxic medication used in several tumor types and also advised in many inflammatory diseases. GIT upsets, alopecia, bone marrow depression and neurotoxicity are its most common adverse effects[16]. In the current study, MTX was taken intraperitoneally at a dose of 0.5 mg/kg twice a week. This dose causes oxidative stress and ROS liberation[12]. Since the central nervous system is extremely vulnerable to attacks by ROS, oxidative stress may result in membrane breakdown and cellular dysfunction with MTX treatment when free radical production exceeds the capacity of antioxidant defense[17].

In the current work, estimation of body weights of rats revealed a statistically significant difference in the body weight between studied groups with the highest weight in the control group and the lowest one in MTX treated group. MTX-treated group showed a highly statistically significant decrease in body weight as compared to the control group. Similar results were reported in previous studies[1´1´12]. Saline-treated rats were found to continue gaining weight over a 4-week period compared to rats that received CMF (cyclophosphamide, MTX, 5-Fluorouracil). This suggests that cytotoxic drugs might influence gastrointestinal function. MTX-induced weight loss could be related to its emetogenic effect, associated vomiting and gastrointestinal toxicity which lead to decreased appetite[20]. Rats of the recovery group in the current study revealed slight gradual improvement in the motor activity. In a previous study, during the treatment period, the general physical activity was significantly decreased in the CMF (cyclophosphamide, MTX,5-Fluorouracil) group as compared to the saline group[19], but when the drugs were discontinued fatigue decreased, indicating that fatigue symptoms are brought on by cytotoxic drugs. It was also reported that motor coordination is affected when Purkinje cells are lost, so motor activity of MTX-treated rats was hampered during Purkinje cell neurodegenerative stages[21]. In this work, TQ co-administration with MTX showed no deterioration of motor activity throughout the experiment. In a preceding study, rats receiving TQ provided substantial protection against motor impairments, and its antioxidant activity may have a protective impact.[22]

H&E-stained sections from albino rats' cerebellar cortex of MTX-treated group showed vacuolated neuropil of the molecular layer. Statistically, this was proved by significant decrease in Purkinje cells number in MTX treated group when compared to other groups. These findings were attributed to the effect of MTX as it increases inflammation, edema and causes tissue necrosis[23]. In addition, Purkinje cells appeared shrunken and deeply stained with pyknotic nuclei in MTX treated group; MTX was reported to cause severe cerebellar cortex damage and Purkinje cell loss[24]. In MTX- treated group, some granule cells appeared shrunken with dark stained nuclei. This was referred to the fact that granule cells have a developmental dependency on Purkinje cells as they are their synaptic target, so, Purkinje cells loss may lead to subsequent granule cell death[25].

Purkinje cell layer showed large pear shaped Purkinje cells arranged in a single raw. Their cytoplasm was basophilic containing pale vesicular nuclei with prominent nucleoli. Granule cell layer contained densely populated small granule cells with deeply stained nuclei surrounded by a thin rim of cytoplasm. Golgi cell with a large pale nucleus was also observed. These results were consistent with those of a previous study in which the authors reported that TQ treatment in rats resulted in decreasing the number of destroyed Purkinje cells and an increase in the number of molecular cells and granule cells[26].

Thymoquinone was found to have a potential effect in preventing apoptosis by regulating mitochondrial pathway[27]. This effect was related to the down regulation of caspase-3, cytochrome-c, cleaved caspase-9 and upregulation of Bcl-2. Bcl-2 protein family plays an important role in apoptotic signal transduction by regulating mitochondrial function. Administration of TQ together with MTX can reverse the adverse effects of MTX on the redox state[28] reported that TQ can scavenge superoxide (O2 −) and hydroxyl radicals (OH•), suppress mRNA expression of the inducible nitric oxide synthase (iNOS) enzyme and enhance the antioxidant enzymes' genes expression, such as catalase (CAT) and glutathione-S-transferase. TQ compounds can act as free oxygen radicals scavengers, increase antioxidant genes expression, such as GSH transferase, GPx, and CAT and inhibite inducible nitric oxide synthase (iNOS) enzyme expression with subsequent inhibition of NO, as well as cyclooxygenase-II and 5-lipoxygenase enzymes production[29]. Furthermore, TQ's high antioxidant abilities were attributed to its structural resemblance to ubiquinone, a natural electron carrier in mitochondria[30].

H&E stained sections from adult male albino rats' cerebellar sections of recovery group showed that some Purkinje cells appeared pyriform with vesicular nuclei and prominent nucleoli, but most cells appeared shrunken with deeply stained pyknotic nuclei. The granule cell layer consists of cells with dark stained nuclei. Generally, signs of cerebellar cortex degeneration were still present, but were less noticeable as those in the MTX-treated group. The toxic cerebellar syndrome caused by MTX and was studied and the authors reported that cerebellar dysfunction symptoms continue up to six months after discontinuation of MTX. These results were morphometrically and statistically proved as the recovery group showed a significant decrease in the mean number of Purkinje cells when compared to the control group[31].

In the present study, the cresyl fast violet stained sections of MTX-treated group showed ill-defined purple Nissl's granules in the perikarya of Purkinje cells. This was proved by the significant difference in the optical density of staining of this group when compared with the control group. This was similar to the findings of a previous study[24]. This reduction was attributed to the substantially reduced Nissl granules by rough endoplasmic reticulum fragmentation and dilation[32]. Moreover, the dilatation of RER was explained by as it was considered as cellular changes preceding apoptosis induced by MTX[13].

On the other side, the cresyl fast violet stained sections of the MTX and TQ treated group showed well-defined purple Nissl granules which appeared as a ring around the nuclei of the Purkinje cells. The concomitant administration of TQ to MTX led to improvement in neuronal function due to oxidative stress suppression, attenuating neurodegeneration, and increased production of ribosomal subunits[11]. These results were also statistically proved as there was no significant difference regarding the optical density of the staining intensity between the MTX and TQ treated group compared to the control group. These findings were attributed these results to TQ anti-inflammatory and immunomodulatory protective effects[11].

Cresyl fast violet stained section of recovery group revealed ill-defined purple Nissl granules in Purkinje cells perikarya, which was statistically proved by significant decrease in the optical density of cresyl fast violet staining when compared to control group indicating that signs of MTX induced oxidative stress still present despite cessation of treatment. In agreement, Yousef *et al*., 2019[13] reported that signs of parotid degeneration in MTX withdrawal group were still present.

In this current work, immuneperoxidase reaction of GFAP was used as it is the predominant intermediate filament in mature astrocytes. Its onset is a marker for astrocyte development and its up regulation is a marker for reactive gliosis[33].

In the present work, the immunoperoxidase reaction for GFAP of the MTX-treated group showed an intense strong positive reaction in the astrocytes processes when compared to the control group. These findings were morphometrically and statistically proved as there was a significant increase in GFAP immunoreaction area percent in MTX treated group when compared with the control group. The intense positive immunoreactive expression of GFAP in the cerebellum of the MTX-treated group was previously described and mentioned that it is released only after cell death or injury[34,35]. It was also stated that gliosis which occurred secondary to drug injury was due to astrocytes activation as a response following neuronal degeneration[36].

In the present work, immunoperoxidase reaction for GFAP of MTX and TQ treated group showed a weak positive reaction in the astrocytes processes as compared to the MTX treated group. This was proved statistically by the significant decrease in GFAP immunoreaction area percent in MTX and TQ treated group as compared to MTX-treated group. Moreover, it was declared that N. sativa seeds extracts had anti-inflammatory effects on the primary glial cells revealed that N. sativa administration resulted in a decreased reactive astrocytes number in experimentally autoimmune encephalomyelitis-induced rats. The N. sativa seed oil contains potent anti-inflammatory compounds[37, 38, 39]. Furthermore, it was recorded that co-administration of TQ with ACR produced a marked decrease in the GFAP content. This is explained by antioxidant activity of thymoquinone against astrocyte damage[22].

In this current study, GFAP-stained sections of the recovery group revealed a strong positive immunoreaction in the cytoplasm and processes of astrocytes. This was verified statistically by a high significant difference between the recovery group and the control group regarding the mean area percentage of GFAP-immunoreaction, indicating that signs of MTX-induced oxidative stress were still present despite cessation of treatment. It was recorded that architecture disturbance did not stop after MTX withdrawal[40].

Bcl-2 plays major roles in the inhibition of the intrinsic apoptotic pathway. Therefore, in this study, Bcl-2 was used as an antiapoptotic marker. Apoptosis is caused mainly by the upregulation of Bax , the pro-apoptotic protein, and the downregulation of the antiapoptotic Bcl-2 proteins.Bcl-2 which is essentially located in the mitochondria[41]. The mRNA expression of Bcl-2 is also tightly correlated with the expression of genes involved in ROS production and detoxification[42].

Immuneperoxidase reaction for Bcl-2 in MTX treated group revealed weak positive immunoreaction in cerebellar cortex. This was statistically proved by the high significant difference between MTX treated group when compared to control group. It was found that there is a negative regulation of the Bcl-2 gene in MTX treated hepatic tissues[43].

The current study proved that TQ co-administration with MTX caused an increase in Bcl2 reaction in cerebellar cortex of MTX and TQ treated group. This result could be explained by the effect of TQ which minimizes the inflammation and the apoptosis process, and its potential impact on the preservation of cerebellar architecture. This finding was statistically verified by the significant increase in Bcl-2 reaction area percentage as compared to MTX -treated group. A former study demonstrated that anti-apoptotic Bcl-2 was enhanced by TQ, so, neuronal apoptosis was prevented by increasing the anti-apoptotic

Bcl-2 protein expression[44]. It was also reported that TQ enhanced the expression of Bcl-2 and decreased Bax level[45]. It was also reported that Bax/Bcl2 ratio significantly decreased when TQ was co-administered with acrylamide (ACR) in comparison with ACR-treated rats[22].

In the current study, the recovery group revealed a weak positive reaction for Bcl-2 in the cytoplasm of nerve cells. There was no significant difference between this group and MTX treated group regarding the mean area percentage of Bcl-2 immunoreaction indicating that signs of MTX-induced oxidative stress are still present. Examination of parotid sections in MTX self-healing group revealed disturbed architecture when compared with the protected group receiving antioxidant drug[13].

Ultrathin sections of the group treated with MTX showed changes in the neuronal structure of Purkinje cells. They showed a reduction in treated size, increased cytoplasmic density with vacuolated areas, and dilatation of RER The nucleus had an irregular indented nuclear envelope and contained condensed chromatin Another study showed that chromatin of Purkinje cell nucleus was fragmented. Their cytoplasm was vacuolated and contained dilated RER and swollen mitochondria[46]. These nuclear alterations were attributed to the antimitotic effect of MTX[47]. Similar description of these results in MTX-treated rats was mentioned [32]. The same authors came to the conclusion that methotrexate is neurotoxic because it significantly altered the ultrastructure of adult male albino rats' cerebella.

Ultrathin sections of MTX treated group revealed some shrunken granule cells with dark stained nuclei, chromatin condensation and vacuolated cytoplasm. These vacuolations might be due to mitochondrial swelling[48]. Another explanation referred these vacuolations to lipid droplets accumulation. These fat droplets resulted from cellular dysfunction and they might coalesce together forming a large vacuole[13].

Ultrathin sections of MTX treated group showed that some nerve fibers of the molecular and granule cell layers showed distortion and dissociation of the myelin sheath. These findings were referred to the persistent dysregulation of oligodendrocytes precursor cell (OPC) population dynamics inhibiting oligodendrogenesis and subsequently leads to demyelination[49]. Another theory was that systemic doses of MTX can cause a long-term decline in the number of oligodendrocytes and a reduced capacity to replenish myelin turnover, which in turn causes a reduction in the degree of myelination[50].

In the current study, the electron microscope examination of MTX and TQ treated group revealed Purkinje cells with euchromatic nuclei and rough endoplasmic reticulum cisternae, mitochondria, and some dilated saccules of perinuclear Golgi. Granule cells contained oval heterochromatic nuclei surrounded by a shell of cytoplasm with free ribosomes and mitochondria. In a previous study, attenuation of the ultrastructural apoptotic changes were observed in the cerebral cortex of Tramadol + Nigella sativa treated rats compared to tramadol treated group. The same author added that most neurons and axons appeared normal with intact mitochondria and rough endoplasmic reticulum[51]. These findings showed that TQ and N. sativa oil prevented cellular apoptosis brought on by tramadol.

These results were also in accordance with[52] in which it was reported that rats treated with TQ revealed minimal histopathological and ultrastructural changes compared with control group. This happens because TQ is a potent antioxidant and free radical scavenger.

Examination of ultrathin sections of the cerebellar cortex of the recovery group showed disruption of myelinated nerve fibers. Purkinje cell had a shrunken irregular nucleus. Its cytoplasm contained dilated RER and numerous cytoplasmic vacuolation. Granule cells appeared with shrunken nuclei. Shrunken glial cells with small necrotic nuclei were observed. Generally, signs of cerebellar cortex degeneration were still present but were less evident than those in the MTX treated group. In another study, the parotid in MTX self-healing group had a markedly disturbed architecture when compared with the group receiving the antioxidant drug[13]. This was explained by the oxidative stress caused by MTX. As oxidant/antioxidant imbalance which resulted causes lipid peroxidation with subsequent organelles and cell membrane lysis.

CONCLUSIONAND RECOMMENDATION:

In conclusion, MTX caused extensive histological, immunohistochemical and ultrastructural alterations in the cerebellar cortex of adult male albino rats establishing its neurotoxicity. Spontaneous recovery from those changes was inadequate. However, co-administration of TQ reduced these alterations proving its neuroprotective action. These experimental results are recommended and should be taken into consideration after accurate studies to estimate the appropriate doses, the target disease and the suitable patient to alleviate MTX neurodegeneration.

CONFLICT OF INTEREST

There are no conflicts of interest.

REFERENCES

1. **Bukowski, K.; Kciuk, M. and Kontek, R. (2020):** Mechanisms of multidrug resistance in cancer chemotherapy. International journal of molecular sciences, 21 (9):1-24.

2. **Katabalo, D. M.; Matinde, R.; Mwita, S.; Marwa, K. and Masalu, N. (2018):** Awareness of chemotherapy side effects and attitude towards chemotherapy use among cancer patients attending oncology clinic at Bugando Medical Centre, in Mwanza, Northern Tanzania. Journal of Drug Delivery and Therapeutics, 8 (5): 448-454.

3. **Younis, N. S.; Elsewedy, H. S.; Shehata, T. M. and Mohamed, M. E. (2021):** geraniol averts methotrexate-induced acute kidney injury via keap1/nrf2/ho-1 and mapk/nf-κb pathways. Current Issues in Molecular Biology, 43 (3): 1741-1755.

4. **Al-Awwad, A. A. and Koriesh, A. (2021):** Cytotoxic Lesion in the Splenium of Corpus Callosum Secondary to Subacute Methotrexate Neurotoxicity. Avicenna Journal of Medicine, 11(3):160-162.

5. **Ebrahimi, R.; Sepand, M. R.; Seyednejad, S. A.; Omidi, A.; Akbariani, M.; Gholami, M. and Sabzevari, O. (2019):** Ellagic acid reduces methotrexate-induced apoptosis and mitochondrial dysfunction via up-regulating Nrf2 expression and inhibiting the IκBα/NFκB in rats. DARU Journal of Pharmaceutical Sciences, 27 (2): 721-733.

6. **Abo-Atya, D. M.; El-Mallah, M. F.; El-Seedi, H. R. and Farag, M. A. (2021):** Novel Prospective of N. sativa Essential Oil Analysis, Culinary and Medicinal Uses.Chapter -9 In Black cumin (Nigella sativa) seeds: Chemistry, Technology, Functionality, and Applications .Springer,cham,Switzerland(pp. 97-129).

7. **Jakaria, M.D.; Cho, D.Y.; Ezazul, H.M.D.; Karthivashan, G.; Kim, I. S.; Ganesan, P. and Choi, D. K. (2018):** Neuropharmacological potential and delivery prospects of thymoquinone for neurological disorders. Oxid Med Cell Longev., 2018:1-17.

8. **Khan, M. A.; Tania, M. and Fu, J. (2019):** Epigenetic role of thymoquinone: impact on cellular mechanism and cancer therapeutics. Drug discovery today, 24 (12): 2315-2322.

9. **Asoom, L. I. A. and Al-Hariri, M. T. (2019):** Cardiac inotropic effect of long-term administration of oral thymoquinone. Evidence-Based Complementary and Alternative Medicine,2019:1-6.

10. **Alkhatib, M.H.; Bawadud, R.S.; Gashlan, H.M. (2020):** Incorporation of docetaxel and thymoquinone in borage nanoemulsion potentiates their antineoplastic activity in breast cancer cells. Sci. Rep, 10: 1–12.

11. **Mahmoud, E. S.; Al-Shahed, F. A. Z. N.; Ouda, E. A. and Al Anany, M. G. (2019):** Effect of thymoquinone on the structure of the cerebral cortex of adult male albino rats treated with tramadol. The Scientific Journal of Al-Azhar Medical Faculty, Girls, 3(1): 97-110.

12. **Felemban, S. G.; Aldubayan, M. A.; Alhowail, A. H. and Almami,I.S . (2020):** Vitamin B17 ameliorates methotrexate-induced reproductive toxicity, oxidative stress, and testicular injury in male rats. Oxidative medicine and cellular longevity, 2020:1-11.

13. **Yousef, D. M.; Abd El-Fatah, S. S.; Al-Semeh, M. D. and Amira, E. (2019):** Oxidative Stress Changes Induced by Methotrexate on Parotid Gland Structure of Adult Male Albino Rat: Can Vitamin C Ameliorate These Changes? The Medical Journal of Cairo University, 87: 2555-2565.

14. **Narayan, J.; Kumar, P.; Gupta, A. and Tiwari, S. (2018):** To compare the blood pressure and heart rate during course of various types of anesthesia in wistar rat: A novel experiences. Asian Journal of Medical Sciences, 9 (6): 37-39.

15. **Dean, A.; Dean, G.; and Colmbier, D. (2000):** Epi-Info Version for the year 2000. Data Base, Statistics and Epidemiology on Microcomputer CDC. Georgia, USA.

16. **Valiev, T. T.; Semenova, V. V.; Ikonnikova, A. Y.; Petrova, A. A.; Belysheva, T. S. and Nasedkina, T. V. (2021):** Role of pharmacogenetic factors in the development of side effects of methotrexate in the treatment of malignant tumors: A review. Journal of Modern Oncology, 23(4), 622-627.

17. **Singh, A.; Kukreti, R.; Saso, L. and Kukreti, S. (2019).** Oxidative stress: a key modulator in neurodegenerative diseases. Molecules, 24 (8):1-20.

18. **Suddek, G. M.; Ashry, N. A. and Gameil, N. M. (2013):** Thymoquinone attenuates cyclophosphamide-induced pulmonary injury in rats. Inflammopharmacology, 21(6): 427-435.

19. **Briones, T. L. and Woods, J. (2011):** Chemotherapy-induced cognitive impairment is associated with decreases in cell proliferation

and histone modifications. BMC neuroscience, 12,124:1-13.

20. **Falvey, S.; Shipman, L.; Ilowite, N. and Beukelman, T. (2017):** Methotrexate-induced nausea in the treatment of juvenile idiopathic arthritis. Pediatric Rheumatology, 15 (1):52.:1-6.

21. **Muñoz-Castañeda, R.; Díaz, D.; Peris, L.; Andrieux, A.; Bosc, C.; Muñoz-Castañeda, J. M. and Weruaga, E. (2018):** Cytoskeleton stability is essential for the integrity of the cerebellum and its motor-and affective-related behaviors. Scientific reports, 8 (1):1-14.

22. **Tabeshpour, J.; Mehri, S.; Abnous, K. and Hosseinzadeh, H. (2020):** Role of oxidative stress, MAPKinase and apoptosis pathways in the protective effects of thymoquinone against acrylamide-induced central nervous system toxicity in rat. Neurochemical research, 45 (2): 254-267.

23. **Jafaripour, L.; Naserzadeh, R.; Alizamani, E.; Javad Mashhadi, S.M.; Moghadam, E.R.; Nouryazdan, N.; Ahmadvand, H. (2021):** Effects of rosmarinic acid on methotrexate-induced nephrotoxicity and hepatotoxicity in wistar rats. Indian J Nephrol, 31(3):218-224.

24. **Vardi, N.; Pinar, H.P. and Ates, B. (2012):** Beneficial effects of chlorogenic acid on methotrexate-induced cerebellar Purkinje cell damage inrats, Journal of Chemical Neuroanatomy, 43: 43-47.

25. **Ahmed, S. M.; Abdelrahman, S. A. and Shalaby, S. M. (2017):** Therapeutic Potential of Mesenchymal Stem Cells vs. Estradiol Benzoate or Avosoya on the Cerebellar Cortex of Ovariectomized Adult Albino Rats. J Cytol Histol,8:1-10.

26. **Kassab, R. B. and El-Hennamy, R. E. (2017):** The role of thymoquinone as a potent antioxidant in ameliorating the neurotoxic effect of sodium arsenate in female rat. Egyptian Journal of Basic and Applied Sciences, 4(3): 160-167.

27. **Ullah, I.; Ullah, N.; Naseer, M. I.; Lee, H. Y. and Kim, M. O. (2012):** Neuroprotection with metformin and thymoquinone against ethanol-induced apoptotic neurodegeneration in prenatal rat cortical neurons. BMC neuroscience, 13 (1): 1-11.

28. **Abdel-Daim, M. M.; Shaheen, H. M.; Abushouk, A. I.; Toraih, E. A.; Fawzy, M. S.; Alansari, W. S. and Bungau, S. (2018):** Thymoquinone and diallyl sulfide protect against fipronil-induced oxidative injury in rats. Environmental Science and Pollution Research, 25 (24): 23909-23916.

29. **Abdel-Daim, M.M.; Abushouk. A.I.; Bungău, S.G.; Bin-Jumah, M.; El-Kott, A.F.; Shati, A.A.; Aleya, L. and Alkahtani, S.(2020):** Protective effects of thymoquinone and diallyl sulphide against malathion-induced toxicity in rats. Environ Sci Pollut Res Int, 27(10):10228-10235.

30. **Alam, M.; Hasan, G. M.; Ansari, M. M.; Sharma, R.; Yadav, D. K. and Hassan, M. I. (2022):** Therapeutic implications and clinical manifestations of thymoquinone. Phytochemistry, 200, 113213.

31. **Kinzel, O.; Verma, R. K.; Wiest, R. and Mattle, H. P. (2015):** Toxic cerebellar syndrome due to methotrexate. Practical Neurology, 15(3), 214–215.

32. **El-ghazouly, D. E. S.; Mahmoud, B. L.; Mansour, M. A. and Konsowa, E. B. (2021):** Histological and Immunohistochemical Study on the Effect of Methotrexate on the Cerebellum of Adult Male Albino Rats and The Possible Protective Role of Lepidium Sativum. Egyptian Journal of Histology, 44 (1): 241-255.

33. **Lin, N. H.; Yang, A. W.; Chang, C. H. and Perng, M. D. (2021):** Elevated GFAP isoform expression promotes protein aggregation and compromises astrocyte function. The FASEB Journal, 35 (5):1-22.

34. **Ahmed, Z. S. O.; Hussein, S.; Ghandour, R. A.; Azouz, A. A. and El-Sakhawy, M. A. (2021):** Evaluation of the effect of methotrexate on the hippocampus, cerebellum, liver, and kidneys of adult male albino rat: histopathological, immunohistochemical and biochemical studies. Acta Histochemica, 123(2):1-13.

35. **Vazi, E. P. G.; Holanda, F.; Santos, N. A.; Cardoso, C. V.; Martins, M. F. M. and Bondan, E. F. (2021):** Short-term systemic methotrexate administration in rats induces astrogliosis and microgliosis. Research in Veterinary Science, 138: 39-48.

36. **Laag, E.M. and Elaziz, H.O.A. (2013):** Effect of aflatoxin-B1 on rat cerebellar cortex: light and electron microscopic study. Egyptian Journal of Histology, 36 (3): 601-610.

37. **El-Haroun, H. (2016):** Comparative study of the possible protective effect of thymoquinone (black seeds) when compared with vitamin E on acrylamide-induced neurotoxicity in the adult guinea pig cerebellar cortex. Egyptian journal of histology, 39 (2): 203-215.

38. **Alemi, M.; Sabouni,F.; Sanjarian, F.; Haghbeen, K.; Ansari, S. (2013):** Anti-inflammatory effect of seeds and callus of Nigella sativa L. extracts on mix glial cells with regard to their thymoquinone content. AAPS Pharm.Sci.Tech, 14:160– 167.

39. **Noor, N.A.; Fahmy, H.M.; Mohammed, F.F.; Elsayed, A.A. and Radwan, N.M. (2015):** Nigella sativa amliorates inflammation and demyelination in the experimental autoimmune encephalomyelitis-induced Wistar rats. Int J Clin Exp Pathol, 8 :6269– 6286.

40. **Tousson, E.; Zaki, Z. T.; Abu-Shaeir, W. A. and Hassan, H. (2014):** Methotrexate-induced hepatic and renal toxicity: role of L-carnitine in treatment. Biomed Biotechnol, 2 (4): 85-92.

41. **Pohl, S. Ö. G.; Agostino, M.; Dharmarajan, A. and Pervaiz, S. (2018):** Cross talk between cellular redox state and the antiapoptotic protein Bcl-2. Antioxidants & Redox Signaling, 29 (13):1215-1236.

42. **Levy, M.A. and Claxton, D.F. (2017):** Therapeutic inhibition of BCL-2 and related family members. Expert Opin Investigat Drugs, 26: 293-301.

43. **Abdel-Wahab, B.A.; Ali, F.E.M.; Alkahtani, S.A.; Alshabi, A.M.; Mahnashi, M.H.; Hassanein, E.H.M. (2020):** Hepatoprotective effect of rebamipide against methotrexate-induced hepatic intoxication: role of Nrf2/GSK-3β, NF-κβ-p65/JAK1/STAT3, and PUMA/Bax/Bcl-2 signaling pathways. Immunopharmacol Immunotoxicol, 42(5):493-503.

44. **Beker, M.; Dallı, T. and Elibol, B. (2018):** Thymoquinone can improve neuronal survival and promote neurogenesis in rat hippocampal neurons. Molecular Nutrition & Food Research, 62 (5):1-10.

45. **Cui, B. W.; Bai, T.; Yang, Y.; Zhang, Y.; Jiang, M.; Yang, H. X. and Nan, J. X. (2019):** Thymoquinone attenuates acetaminophen overdose-induced acute liver injury and inflammation via regulation of JNK and AMPK signaling pathway. The American Journal of Chinese Medicine, 47 (3): 577-594.

46. **Salwa, M. O.; Dorreia, A.; Ahlam, W. M. and Wail, M. (2021):** Toxic Effects of Methotrexate on the Cerebellar Cortex of Adult Albino Rats and the Possible Protective Role of Vitamin C: An Electron Microscopic Study. The Medical Journal of Cairo University, 89, 2043-2047.

47. **Ozkorkmaz, E.G; Gul, N.; Ozluk, A. and Ozay, Y. (2018):** Ultrastructural alterations of liver tissue cells in methotrexate-treated balb/c mice. J Microsc Ultrastructure, 6 (4):192-196.

48. **Lombaert, I.M.; Brunsting, J.F.; Wierenga, P.K.; Kampinga, H.H.; De Haan, G. and Coppes, R.P. (2008):** Cytokine treatment improves parenchymal and vascular damage of salivary glands after irradiation. Clin. Cancer Research, 14 (23): 7741-7750.

49. **Geraghty, A. C.; Gibson, E. M.; Ghanem, R. A.; Greene, J. J.; Ocampo, A.; Goldstein, A. K. and Monje, M. (2019):** Loss of adaptive myelination contributes to methotrexate chemotherapy-related cognitive impairment. Neuron, 103 (2): 250-265.

50. **Berlin, C.; Lange, K.; Lekaye, H. C.; Hopland, K.; Phillips, S.; Piao, J., and Tabar, V. (2020):** Long-term clinically relevant rodent model of methotrexate-induced cognitive impairment. Neuro-oncology, 22 (8):1126-1137.

51. **Omar, N.M. (2016):** Nigella sativa oil alleviates ultrastructural alterations induced by tramadol in rat motor cerebral cortex. J Microsc Ultrastruct. ,4(2):76-84.

52. **Hassanein, K. M. and El-Amir, Y. O. (2018):** Ameliorative effects of thymoquinone on titanium dioxide nanoparticles induced acute toxicity in rats. International journal of veterinary science and medicine, 6(1), 16-21.

الملخص العربى

تأثير الميثوتريكسيت علي قشرة المخيخ لذكورالجرذان البيضاء البالغة والدورالوقائي المحتمل للثيموكوينون

(دراسة هستولوجية و هستوكيميائية مناعية)

عزة سعد شحاتة, سمر محمود الوكيل, سماح محمد أحمد, مها زايد محمد

قسم الأنسجة الطبية وبيولوجيا الخلية ـ كلية الطب ـ جامعة الزقازيق

الخلفية: الميثوتريكسات هو أحد مضادات الأيض الأكثر شيوعًا في العلاج الكيميائي ومثبط المناعة في أمراض المناعة الذاتية، وهو أحد الخيارات الرئيسية لعلاج أنواع مختلفة من السرطانات، والثيموكينون هو المكون الرئيسي لـحبة البركة و له استخدامات علاجية بارزة حيث أنه مضاد للالتهاب ، ومضاد للأكسدة ، والميكروبات ، وله تأثيروقائى على الكبد.

الهدف: هدفت هذه الدراسة إلى توضيح تأثيرالثيموكينون على التغيرات النسيجية لقشرة المخيخ في ذكور الجرذان البيضاء المعالجة بالميثوتريكسات بالإضافة إلى ذلك تقييم استعادة التركيب النسيجي الطبيعي بعد توقف الميثوتريكسات.

المواد والطرق: تم تقسيم ستة وثلاثين من ذكور الجرذان البيضاء الأصحاء إلى أربع مجموعات: المجموعة الأولى (المجموعة الضابطة)، المجموعة الثانية (مجموعة الميثوتريكسات) أعطيت (٠,٥ مجم / كجم من وزن الجسم) ميثوتريكسات داخل الصفاق مرتين في الأسبوع لمدة أربعة أسابيع. أما المجموعة الثالثة (مجموعة الميثوتريكسات و الثيموكينون) فحقنت بالميثوتريكسات داخل الصفاق بجرعة مشابهًة للمجموعة السابقة بالتزامن مع الثيموكينون عن طريق الفم بجرعة (١٠ مجم / كجم من وزن الجسم يوميًا) لمدة أربعة أسابيع، والمجموعة الرابعة (مجموعة الاسترداد) تلقت الميثوتريكسات داخل الصفاق مثل المجموعة الثانية ثم تركت المجموعات دون علاج لمدة ١٥ يومًا. وفي نهاية التجربة ، خدرت جميع الفئران وتم الحصول على عينات من المخيخ ومعالجتها للفحص بالمجهرين الضوئى و الإلكتروني النافذ. ثم أجريت التحليلات المورفومترية والإحصائية.

النتائج: خلال التجربة اظهرت مجموعة الميثوتريكسات تدهورا تدريجيا في النشاط الحركي وانخفاضا ذو دلالة إحصائية في وزن الجسم ، و أظهر الفحص المجهري خلايا بركنجي منكمشة و محتوية على أنوية داكنة، و أظهرت صبغة كريسيل البنفسجية حبيبات نسل غير واضحة المعالم في سيتوبلام خلايا بركينجي والخلايا العصبية الأخرى، و أظهرت المقاطع المصبوغة بالصبغة الهستوكيميائبة المناعية لـ GFAP تفاعلًا إيجابيًا قويًا في الخلايا النجمية ، ولون باهت (إيجابي ضعيف) لـ Bcl2 في سيتوبلازم الخلايا العصبية. أما المجموعة المعالجة بـالميثوتريكسات و الثيموكينون فلم يظهربها أي تدهور في الأنشطة الحركية ومجهريا كان لمعظم خلايا بركنجي شكل كمثري ونواة حويصلية وسيتوبلازم قاعدى و ظهرت بعض خلايا بركنجي غير منتظمة و داكنة، و كانت علامات التنكس لا تزال موجودة في القشرة المخيخية لمجموعة الاسترداد.

الخلاصة: أظهرت قشرة المخيخ في الفئران البيضاء المعالجة بـالميثوتريكسات اختلافات هستولوجية واضحة تم ملاحظتها بواسطة المجهرين الضوئي والإلكتروني، وأيضاً كان هناك تغيرات ملحوظة في التفاعلات الكيميائية الهيستولوجية المناعية مما يشير إلى أنه يسبب تسمما بالخلايا العصبية، و خفف من هذه التأثيرات إعطاء الثيموكينون الذى كان تأثيره أقوى من التوقف عن إعطاء الميثوتريكسات فى مجموعة الإسترداد مما يشير إلى تأثير الثيموكينون الفعال على التركيب الهستولوجى العصبي، وذلك يمكن أخذه فى الإعتبار إكلينيكيا.